Improving the Thermal Performance of Rotary and Linear Air-Cored Permanent Magnet Machines for Direct Drive Wind and Wave Energy Applications

Improving the Thermal Performance of Rotary and Linear Air-Cored Permanent Magnet Machines for Direct Drive Wind and Wave Energy Applications

Markus A. Mueller, Joseph Burchell, Yew Chuan Chong, Ozan Keysan, Alasdair McDonald, Mike Galbraith, Estanislao J.P. Echenique Subiabre

***Abstract*—Air-cored machines offer benefits in terms the elimination of magnetic attraction forces between stator and rotor. With no iron in the stator there is not a good thermal conduction path for heat generated by Joule losses in the stator winding. Results from both models and experimental tests are provided in this paper to investigate different methods of cooling air-cored windings, including natural air-cooling, direct liquid cooling and the use of heat pipes.**

***Index Terms*— PM machines, direct drive, air-cored windings, wind energy, wave energy, linear machines, thermal performance**

I. Introduction

AIR-CORED winding machines have been proposed for small wind applications of typically less than 20 kW [1 & 2]. These machines are typically axial flux machines with the winding sandwiched between two permanent magnet discs. Compared to an iron cored machine the magnetic gap is larger, and hence air cored machines exhibit lower magnetic loading. However, the lack of iron in the winding reduces weight, eliminates iron loss, and there are no magnetic attraction forces between the stator winding and the permanent magnet rotor, making assembly easier than in a conventional iron cored machine. Thermal performance in an air-cored machine is challenging due to the loss mechanism and the material used. Copper losses and eddy current losses in the windings dominate the loss mechanism in air-cored machines. The coils tend to be potted in epoxy to provide support, but the epoxy materials used tend to have poor thermal characteristics. Although the lack of iron has some advantages, an air-cored winding does not have a good thermal conduction path to dissipate the heat to the outer surface of the machine in the same way as the stator iron core pack does in iron cored machines. The copper coils themselves conduct heat away, and convection becomes more important. Also the reduction in magnetic loading in air-cored machines can be compensated for by an increase in electric loading, but this leads to an increase in copper losses, and hence thermal issues. Air-cored machines tend to be of a discoid structure, which limits the diameter due to large forces acting between the magnet discs. A novel modular air-cored PM machine, is demonstrated in [3], which is suitable for large diameter machines in direct-drive wind energy applications, and is branded as the C-GEN machine in [4]. Due to its modular nature C-GEN lends itself to linear machines for direct drive wave energy applications. The thermal performance of windings in the C-GEN topology is the focus of the investigation in this paper. For direct drive linear machines the thermal performance is even more challenging than in a rotary machine because the airgap velocity is of the order of 1 m/s, as shown in [4]. In direct drive rotary machines the low rpm can be compensated for by increasing the machine airgap diameter resulting in larger airgap velocities, which provide more air-flow within the airgap aiding convection. Experimental and modelling techniques will be used to demonstrate improved methods of cooling in air-cored windings in multi-stage axial flux machines and linear machines.

II. C-GEN AIR-CORED TOPOLOGY

In its simplest form the C-GEN permanent magnet (PM) generator technology consists of a double sided permanent magnet rotor sandwiching an air-cored winding. The topology can be radial or axial machines. In order to enable scaling to large diameters each magnet pair is modified into a c-core as shown in Fig. 1, forming the most basic rotor module. The winding consists of concentrated coils, with the most basic module consisting of a single coil potted in epoxy, also shown in Fig. 1. A machine can be built from a number of c-cores to give a radial flux machine as shown in Fig. 2, or mounted in the axial and circumferential direction to form a module as shown in Fig. 3(a), which when combined with other similar modules produce a multistage axial flux machine Fig. 3(b). The modules are bolted onto a support structure. In this example there are 3 stages. All the magnetic forces are reacted locally within the c-core, so the structure has to support the weight only. Rather than have a single potted coil a number of coils can be potted together forming a so-called stator blade. In Fig. 3(c) each blade has three coils, one for each phase. These blades are inserted into the c-core modules to produce the finished machine, Fig. 3(d). Since there is no iron within the stator blade there are no magnetic forces between the stator blade and the PM rotor module, making assembly straightforward. The modular c-core, combined with the air-cored winding, enables scale up to large diameter and hence multi-MW direct drive generators, with the major benefit in final assembly. Assembly of such a machine at large diameter has been demonstrated by McDonald et al [5], a 1 MW machine at 6.5 m diameter operating at 13 rpm consisted of 22 stator and rotor modules, Fig. 4. C-GEN modules can be arranged to form a linear machine as shown in Fig. 5. The design details of this linear machine can be found in reference [4].

M. A Mueller is with the School of Engineering, Institute for Energy Systems at the University of Edinburgh, UK, (Markus.Mueller@ed.ac.uk
J. Burchell is with the School of Engineering, Institute for Energy Systems at the University of Edinburgh, UK (J.Burchell@ed.ac.uk)
Yew Chuan Chong is with Motor Design Ltd, Edison Court, 5 Wrexham Technology Park, Wrexham LL13 7YT, UK (cychuan_clk@hotmail.com)
Ozan Keysan, is with the Middle Eastern Technical University, Ankara, Turkey. (keysan@metu.edu.tr)
A.McDonald is with the Dept. of Electrical and Electronic Engineering, University of Strathclyde, Glasgow, UK (Alasdair.McDonald@strath.ac.uk)
M. Galbraith is with Fountain Design Ltd, County Durham, UK, (MikeG@fountaindesign.co.uk)
J.P. Echenique Subiabre is with the School of Engineering, Institute for Energy Systems at the University of Edinburgh, UK (E.Echenique-Subiabre@ed.ac.uk)

Figure 1. Single c-core and coil

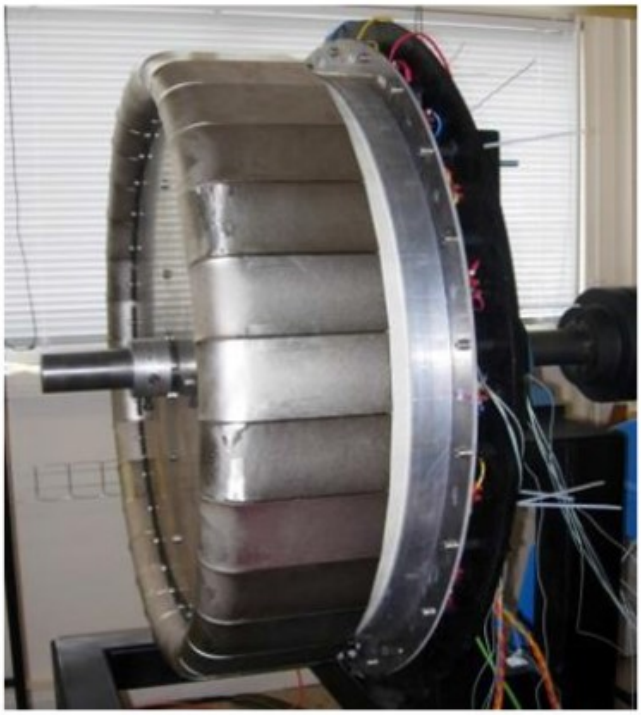

Figure 2. 15 kW Prototype with c-core modules

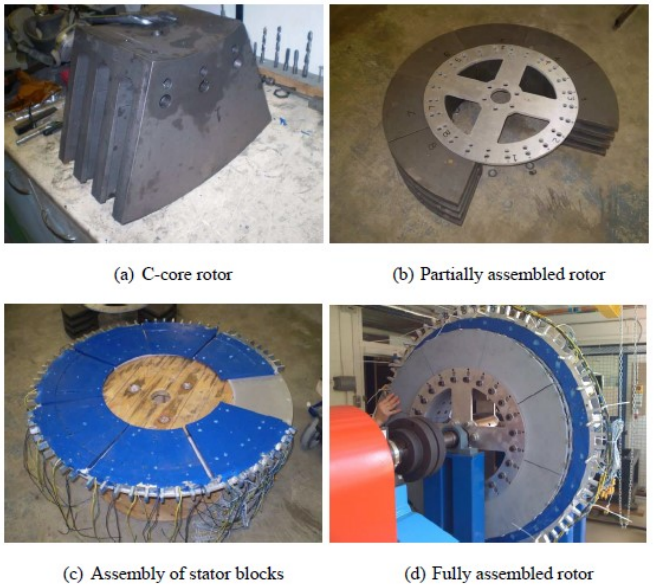

(a) C-core rotor (b) Partially assembled rotor

(c) Assembly of stator blocks (d) Fully assembled rotor

Figure 3. 25 kW multistage axial flux machine

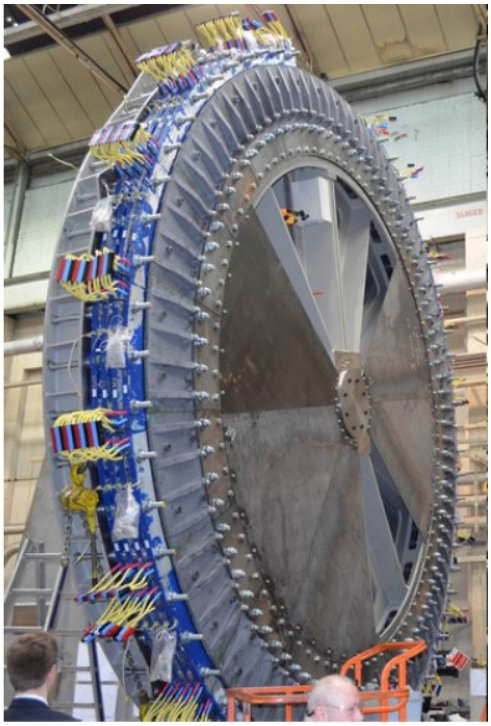

Figure 4. 1 MW Demonstrator, 13 rpm, 6.5m diameter

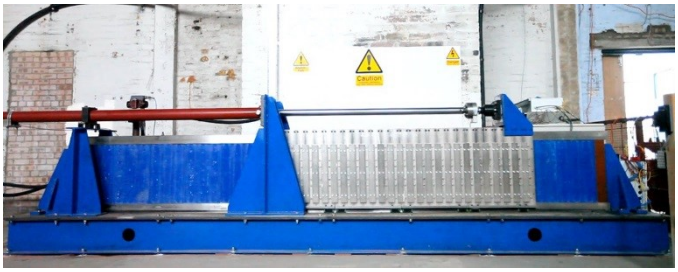

Figure 5. 50 kW Linear Prototype

III. MULTI-STAGE AXIAL FLUX MACHINE

A 3-stage rotary axial flux machine is shown in Fig. 3. This prototype rated at 25 kW at 100 rpm was used as a test platform, in which individual design changes could be made to modules to show the impact of the various changes made. In this investigation three design changes were investigated with respect to thermal performance: Vent Holes in the PM rotor modules; coil module surface topology; and the use of heat pipes within the stator blades. Both experimental and Computational Fluid Dynamics (CFD) results are presented.

A. Vent Holes

The prototype is ventilated by 24 radial and axial holes respectively on the rotor at the inner radius as illustrated in Fig. 6. The outer edge of the machine is unshrouded. Both axial and radial holes have the same diameter of 20 mm, and the axial holes are located at a radius of 272 mm. Different arrangements of the air inlet holes can be tested by blocking the unnecessary holes using tape. Three cases were considered:

1. All holes unblocked.
2. Only radial holes unblocked.
3. Only axial holes unblocked.

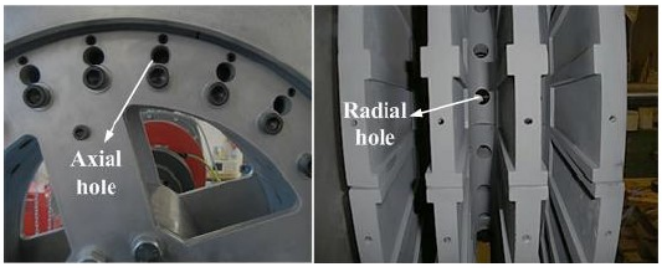

Figure 6. Location of vent holes

1) Electrical Losses

In an air-cored machine electrical losses in the stator winding dominate, which can be divided into no-load and load losses. No-load losses are caused by the action of the rotating field of the magnets inducing eddy and circulating currents in the coils. The phase current produces copper loss in the windings. Armature reaction produces losses in the rotor in the iron core and the permanent magnets. Determination of these losses is described in detail in [6], and summarized here for completeness sake.

Copper and rotor losses are calculated using equation (1):

$$P_{Cu} = 3I_{rms}^2 R_{Cu}^{amb}(1 + \alpha_{Cu}\Delta T_{coil}) \quad (1)$$

In this case the machine is loaded with a resistive load, so that the rms phase current can easily be calculated from the induced emf and phase impedance.

Eddy and circulating current losses were determined by no-load tests from standstill to rated speed. Torque input and mechanical speed were measured at the shaft of the generator in steady-state conditions. At low speed, the mechanical losses are linearly proportional to the rotational speed, whereas eddy and circulating current losses are directly proportional to the square of rotational speed according to equations (2) & (3):

$$P_{mech-loss} = k_m \omega_m \quad (2)$$

$$P_w = (k_{eddy} + k_{circ})\omega_m^2 \quad (3)$$

Segregation between eddy and circulating current losses is possible by performing the no-load test twice: with disconnected coils and parallel connection. Unfortunately, the mechanical losses increase when the circulating current is flowing into the windings due to the effects of an unwanted ripple in the torque. Nevertheless, the authors assumed that, at low speed, the mechanical losses have no impact on the heat generation. Table I summarizes the experimental constants for the no-load losses. The eddy and circulating current losses at 100 rpm are 64.7 W and 217.5 W, respectively.

TABLE I
EXPERIMENTALLY DERIVED LOSS CONSTANTS
MECHANICAL, EDDY, AND CIRCULATING CURRENT LOSSES OF THE AFPM GENERATOR AT RATED SPEED

	Disconnected coils (no circulating loss)			Parallel Connection	
	k_m	k_{eddy}	k_{eddy} (Analytical)	k_{eddy}	k_{circ}
Constants at 21.8°C	0.171	0.589	0.583	0.589	1.980
Power Loss at 100rpm (W)	1.8	64.7	63.9	64.7	217.5

Rotor losses due to eddy currents are difficult to estimate analytically, and most of the literature on AFPM machines does not consider these losses in low-speed machines. Hence the core resistance was measured using the direct-axis connection described in [7], with a magnetic analyzer (Wayne Kerr Electronics, model 3260B), that gives the equivalent impedance in the locked-rotor test. It is assumed that the equivalent rotor core resistance is not affected by temperature because the resistivity coefficients are orders of magnitude less than that for copper. Equation (4) can then be used to calculate the rotor loss:

$$P_{rotor} = 3I_{rms}^2 R_{core} \quad (4)$$

At ambient temperature, eddy current, circulating current and copper losses in the windings contribute approximately 84% of total electrical losses. The power losses in the rotor are smaller than those in the stator. The reaction field from the winding creates asynchronous time varying fluxes on the rotor causing eddy current losses in the magnets and the iron supporting them. At rated speed, the rotor losses account for only 16% of the total electrical losses at ambient temperature. A breakdown of the electrical losses at 100 rpm is shown in Fig. 7 calculated using the method outlined in [6]. The copper loss is the major loss accounting for 71% of the total electrical losses, whereas the eddy current loss in the windings represents only 3% of the total losses. It can be seen that the coil temperature rise only gives significant influence to the copper loss and circulating current loss as the resistivity of the copper increases with temperature.

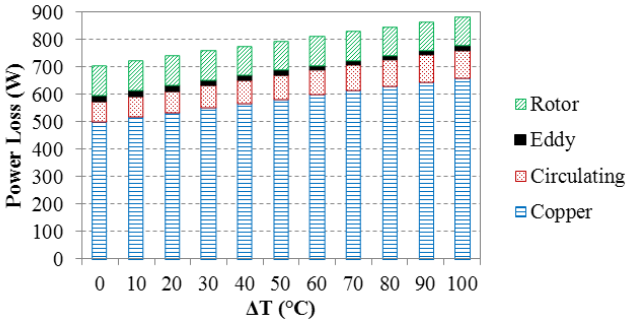

Figure 7. Loss breakdown for 25 kW prototype

2) CFD Modelling

Fig. 8 shows the dynamic integration between the input losses and CFD. The CFD model updates the steady state input loss in each iteration until the temperature of the coil converges.

CFD modelling was conducting using commercially available software Star CCM [8], with full details provided in reference [9].

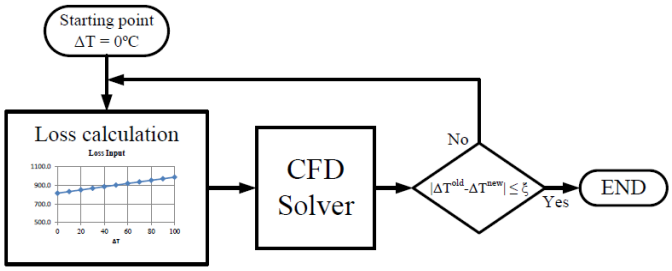

Figure 8. Schematic of integrated loss-CFD model.

Results of temperature from the CFD modelling are shown in Fig. 9 for the three different cases. As might be expected the temperature increases as the vent holes are blocked up, such that with axial holes only the maximum temperature is in the region of 106 ºC.

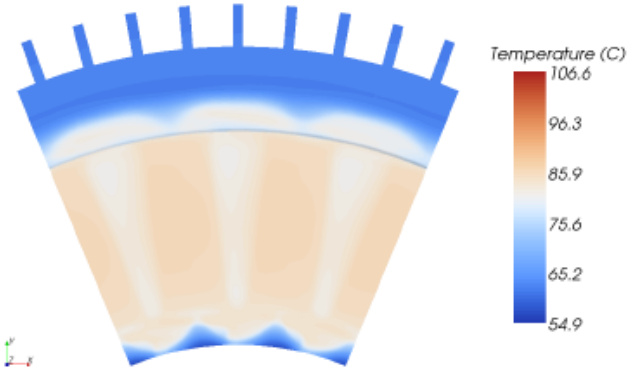

(a) Case 1: Ventilation with radial and axial holes

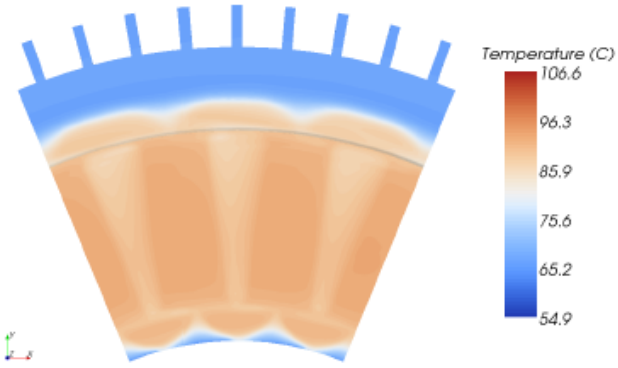

(b) Case 2: Ventilation with radial holes only

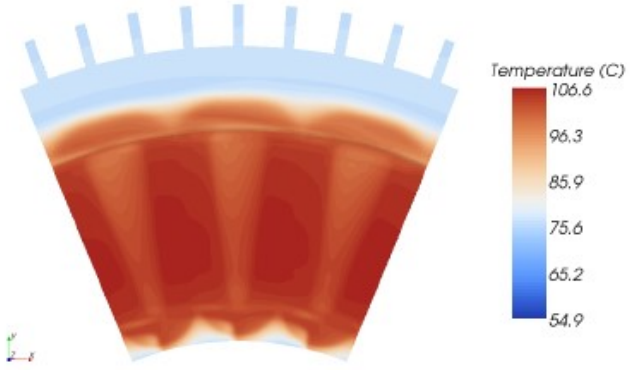

(c) Case 3: Ventilation with axial holes only

Figure 9. Temperature distribution for Cases 1 to 3.

3) Experimental Tests

Since copper loss is the major loss component in this machine topology, the temperature rise of stator coils was recorded during the tests. The temperature is measured using type K thermocouple. The measurement range is from -100 °C to 250 °C with an accuracy of ±1.5 °C. Thermocouples were embedded in the stator to measure the local temperatures at the coils. Thermocouples A, B, and C measure the coil surface temperature at the outer radius, mid and inner radius respectively as shown in Fig. 10. Four coils were monitored and each coil is located at a different angle in the stator disc. No significant difference in temperature rise was found between the coils. The experimental heating curves are illustrated in Fig. 11. The heating curves of thermocouple A, B and C are taking the averaged value of those four coils. Since the generator is stator-critical, temperature measurement was not performed on the rotor. The machine was warmed up at full load before the ventilation tests were carried out until steady-state was achieved. There was an interval of 20 minute. The heating curve profiles for the warm-up period in Fig. 11(a) and Fig. 11(b) are different because in Fig. 11(b) the generator was warmed up with all the ventilation holes blocked, whereas in Fig. 11(a) the ventilation holes are unblocked. This does not affect the ventilation tests conducted after the warm-up period. The measured temperature rise is shown in Table II. More details of the experimental work and additional results can be found in reference 8.

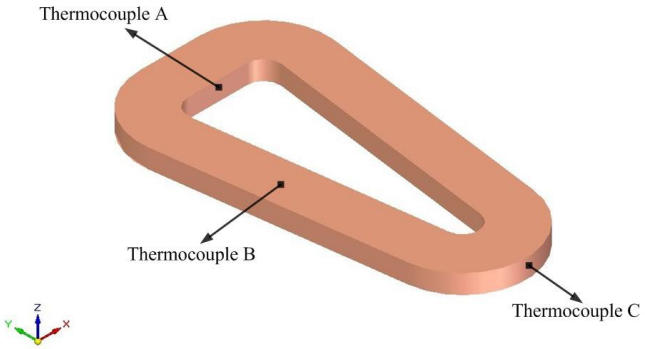

Figure 10. Location of thermocouples

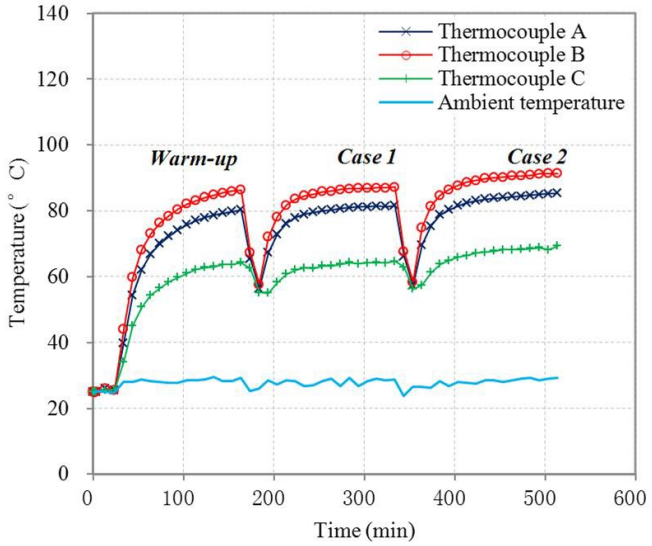

Figure 11(a). Warm-up holes unblocked

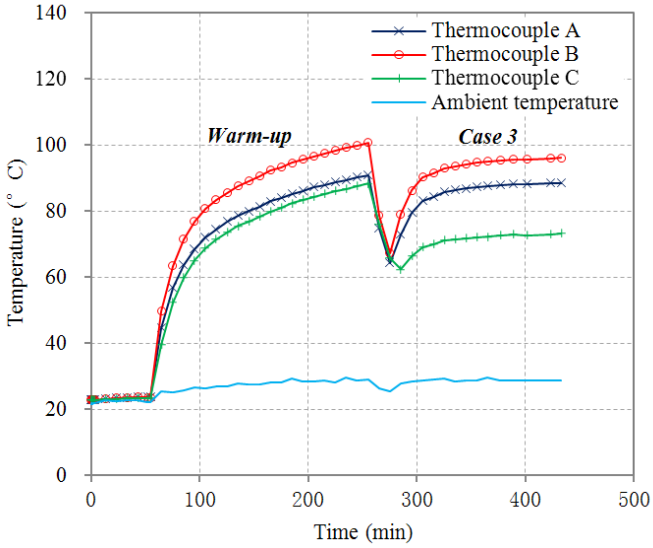

Figure 11(b). Warm-up holes blocked

TABLE II
MEASURED TEMPERATURE RISE

Temperature Rise	Case 1: Ventilation with radial and axial holes	Case 2: Ventilation with radial holes only	Case 3: Ventilation with axial holes only
Thermocouple A	52.6°C	56.4°C	59.5°C
Thermocouple B	58.2°C	62.4°C	67.0°C
Thermocouple C	35.6°C	40.3°C	44.1°C

B. Coil Module Surface Topology

Coil module topology was varied within one stage. 6 coils were supported in 4 different ways as shown in Fig. 12: Type A: coils simply supported with no epoxy; Type B: coils potted in epoxy but with the former removed; Type C: coils potted entirely in epoxy; Type D: Coils potted in epoxy with the former removed and metal clamp holding coils at the end. As can be seen the results show that Type A is the best structure because all of the copper is exposed to the airflow. Removing the former produces additional turbulence in the airgap, providing better convective heat transfer. As expected the best performing coil is Type A, in which the cooling air is in direct contact with the copper coils. The rough surface induces turbulence improving the cooling performance. Although Type D has similar performance once the steady state is achieved. The lack of former induces turbulence in type D, but also heat is conducted down the copper to the metal coil clamping plate coupled to the finned outer ring.

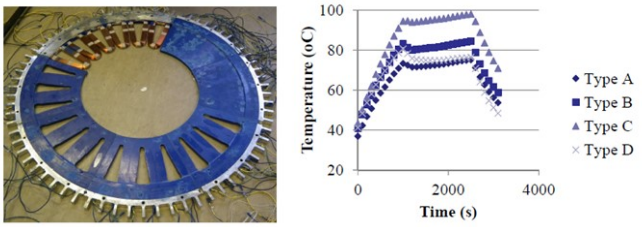

Figure 12. Coil Surface Topology and Results

C. Heat Pipes

Heat pipes were installed at various positions in the coil modules as shown in the actual coils in Fig. 13. Experimental results of temperature (to be presented in the main paper) show that Bend Pipes produce a 20% reduction in temperature compared to a module with no heat pipes. All modules were installed on the 25 kW prototype, shown in Fig. 3(d). The four modules were inserted alongside standard modules with no heat pipes allowing direct comparison of thermal performance. Tests were performed at full load and no load.

1) Full Load Test.

With the generator rotating at 100 rpm the coil modules making up one stage were loaded at 8 kW, the rating per machine stage. During the heat run test the coil temperatures were recorded at regular time intervals up to the steady state. Table III summarises the maximum temperature values for all coils and heat pipe locations. Red highlight is used to show the maximum temperature for a particular thermocouple location and green the minimum. In this case the module with bend pipes at the top has performed overall better than the other modules, and 10-15 °C better than coils 17 & 16 with no heat pipes in thermocouple location TC. The short pipes have no impact at all in the load tests. The TD result for coil 23 looks like an anomaly. The TC thermocouple in coil 1 is not close to a long heat pipe, and so the temperature is expected to be higher than for coils 2 & 3.

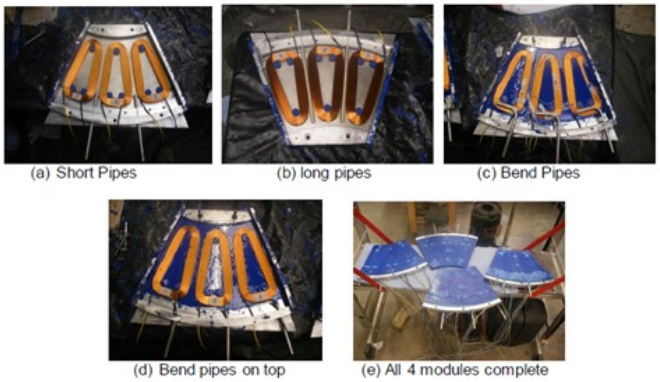

Figure 13. Location of heat pipes

TABLE III
HEAT PIPE RESULTS AT FULL LOAD

Location	Max. Coil Temp (^{O}C)													
	No heat pipes		Short pipes			Long pipes			Bend pipes			Bend pipes at top		
	17	16	22	23	24	01	02	03	04	05	06	07	08	09
TA	34.0	34.1	-	37.9	-	-	42.7	-	-	35.4	-	-	32.7	-
TB	58.5	-	-	86.8	-	-	66.4	-	-	54.0	-	-	53.6	-
TC	70.4	68.2	83.5	90.2	92.0	84.3	68.6	66.5	-	60.0		56.6	55.9	54.8
TD	67.2	56.7	-	43.3	-	-	60.2	-	-	53.9	-	-	54.6	-

Using the results from the bend pipes at the top, there is approximately a 20% reduction in temperature of the main part of the winding. An increase in current of 11% would bring the temperature back up to the original value, leading to an 11% increase in torque output for the same generator mass and volume. If the machine were operated at the same torque but with 11% more current, the magnetic field could be reduced leading to less magnet material and lower cost. The reduction in magnet material would be less than 11%.

2) No Load Tests

The no load test was performed to investigate if eddy currents were induced in the heat pipes, but the tests also measured the temperature rise due to eddy currents induced in the coils themselves. After 2-3 hours of operation the temperature in the thermocouple locations only rose by about 3-4 ºC above ambient. Hence it can be concluded that eddy currents in both the coils and the heat pipes is not an issue.

IV. Linear Generator

In [4] a 50 kW C-GEN linear prototype was designed, built and tested. Fig. 5 shows a photo of the completed machine. The machine was rated at 50 kW at a peak velocity of 2 m/s. Due to the limitations of the test rig only a peak of 1.2 m/s could be achieved. When the machine was loaded at even ½ and ¾ load it was clear that there was a thermal problem. The machine was naturally air-cooled, but because of the low linear velocity there was little air flow within the airgap of the machine. As shown in section III B the encapsulation of the coils with epoxy or not has a noticeable effect on the cooling. The surface topology of the coils affects the degree of air mixing within the airgap. In Fig. 14 the stator and rotor surface topologies can be either smooth or salient. For completely smooth surfaces the airflow is close to laminar, but with a salient surface, in this case the PM translator, the movement of the magnets induces turbulence and thus more air mixing.

Optimising the airgap geometry for improved heat transfer in a fully flooded generator is not the only option for passive cooling. In the airgap the air-cored coils are in direct contact with the fluid, but the heat is also conducted through the copper coils, as it is a very good thermal conductor. External passive cooling can also be provided by arranging the position of the coils and translator, such that the coils are externally mounted with respect to the translator as shown in Fig. 15(a). For comparison a fully enclosed concept is shown in Fig. 15(b), which in terms of passive cooling is the worst case scenario. The 50 kW machine had a salient PM topology, smooth epoxy encapsulated stator windings, and was fully enclosed (Fig. 15(b)). Passive cooling for this machine was always going to be challenging. In this work a fully enclosed C-GEN linear generator topology was investigated with different stator and rotor surface topologies. Both passive air and water cooled systems were considered. Experimental results have been presented to demonstrate the impact of the various design combinations and with different fluids.

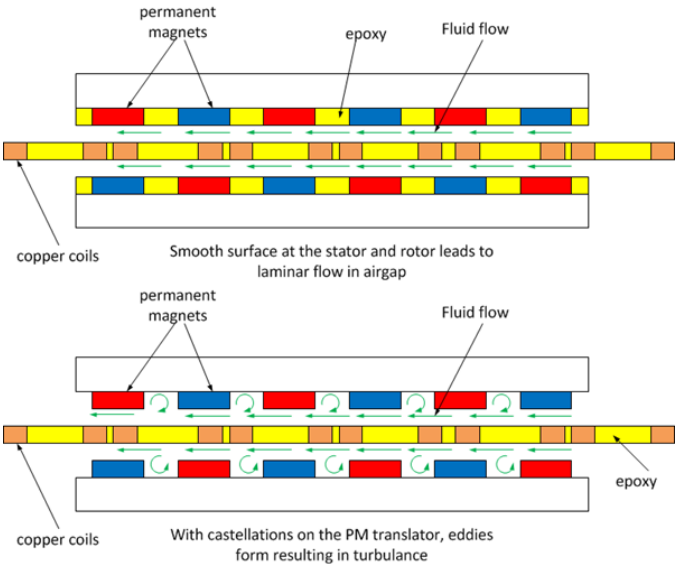

Figure 14. Stator and rotor surface topologies

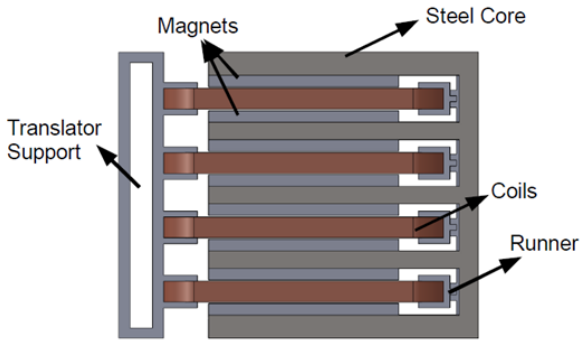

Figure 15(a). Open-ended external support of Stator Coil Modules

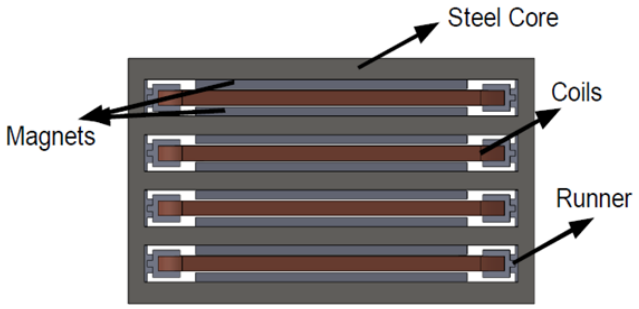

Figure 15(b). Fully Enclosed Stator Coil Modules

A test rig (Fig. 16) was developed to investigate the airgap surface topology of the closed C-GEN linear machine, in which the PM translator was salient, and different winding topologies could be tested. The test rig was designed for both air and water cooling. Fig. 17 shows three different coil samples: sample A shows enameled coils with tape insulation; sample B shows coils fully epoxied; and sample C shows coils potted in epoxy but with the former removed.

Figure 16. Linear test rig for testing thermal performance

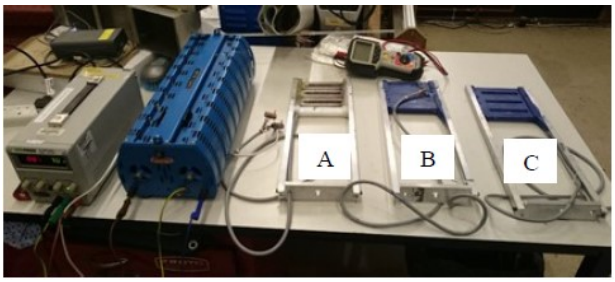

Figure 17. Coil samples A, B & C

Each coil sample was tested as follows:

1. Stationary in air with dc current from 1 A to 8 A. per coil.
2. Stationary in flooded tank with dc current from 1 A to 8 A per coil.
3. Running flooded in the tank with dc current at 4 A and 6 A per coil.

Fig. 18 to 20 show the temperature results for tests 1 & 2 with 3 A per coil. In each test the temperature was allowed to rise to close to an equilibrium value, and it can clearly be seen that operating in water has a significant thermal impact on the coils. All coil types perform similarly when stationary.

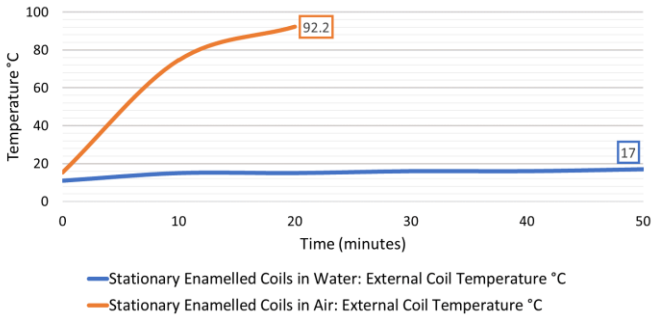

Figure 18. Sample A, Enamelled coils, 3 A/coil

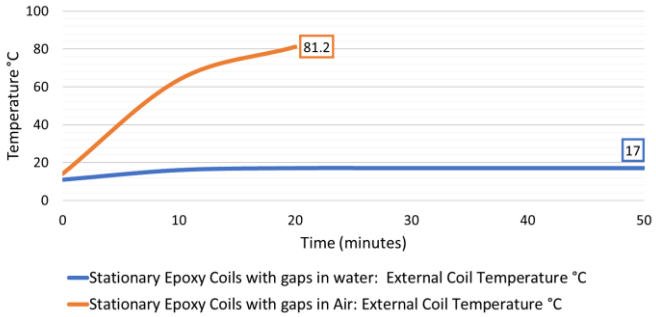

Figure 19. Sample B, Epoxied coils, 3 A/coil

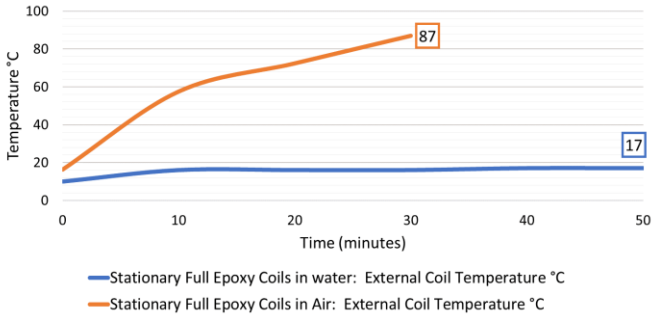

Figure 20. Sample C, Epoxied coils with gaps, 3 A/coil

Fig. 21 shows the effect of moving the translator on the winding temperature when operating wet (Test 3) with a coil current of 8 A. The dotted line shows the point at which movement was initiated. For all coil samples the temperature reduces after the translator starts to move, and the decrease in temperature depends upon the velocity of the translator. The results indicate that the enameled coils perform best when stationary and moving for all currents. The surface around the bare enameled coils will be rougher than the epoxy potted coils, resulting in more turbulence.

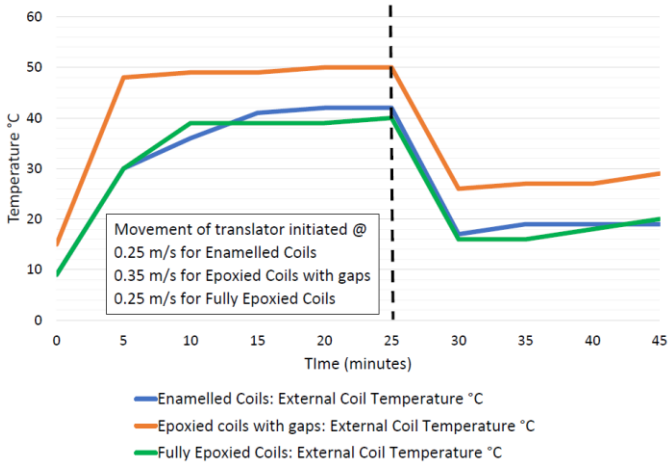

Figure 21. Movement with 8 A/coil

V. Discussion

Air-cored machines have advantages over iron-cored machines in terms of assembly, which for large diameter machines in direct drive systems is significant. However, the lack of a good heat conduction path makes cooling a challenge. In this paper a number of different methods of cooling have been explored, all passive techniques. In axial flux machines improved air-cooling is obtained using axial and radial vent holes. Radial vent holes have more of an impact than axial holes. The radial holes draw air in, which flows radially across the coils providing direct cooling contact. Air from the axial holes has to turn a corner before moving radially, diminishing the impact. Air-cored coils tend to be potted in epoxy to provide structure, but the epoxy does not have good thermal characteristics. In section III B the coil surface topology is investigated, and enameled coils with no epoxy provide the best performance, as the cooling air is coming into direct contact with the heat source, namely the copper windings. Heat pipes were investigated in section III C. The heat pipes were positioned in various locations with the coil modules, and as expected the long heat pipe close to main part of the coil proved best. Overall for the axial flux machine the combination of vent holes and heat pipes gave the best cooling. In the linear machine the velocity is very low typically 1m/s or less, and hence there is not much air flow. Turbulence can be induced by ensuring there are salient surfaces in the airgap to provide more mixing of the air. However, even with induced turbulence the temperature rise is still high. Flooding the machine completely makes a significant difference, as shown in Fig. 18-20. The impact of movement is demonstrated in Fig. 21, with a reduction in temperature of 21 ºC from stationary. With natural air cooled machines a current density of 4 A/mm^2 is typical, but results from the mini test rig suggest that more than 18 A/mm^2 could be achieved (wire diameter is 0.75 mm, at a current of 8 A). As a result of this improved cooling the power density could be increased by about a factor of 5, which will reduce material costs per kg, but at the expense of efficiency. Although higher current densities could be used and thus increase power density, the resulting reduction in efficiency may not be worth it. A balance is required which requires design optimisation. However, the results indicate that the generator could withstand an extreme condition, such as a short circuit condition, where such high current densities would be experienced. In a marine application survivability is key, and tends to dominate the design. Hence it would be expected that flooded air-cored machines would operate at normal current densities, but with an extended range for survivability.

VI. Conclusion

A number of methods have been investigated for improving the cooling of air-cored machines used for direct drive applications. Based on the results presented in this paper air-cooling in rotary machines is sufficient with a combination of radial vent holes, long heat pipes and coils with no epoxy. For marine applications it is recommended that the winding is fully flooded, not only for normal operating conditions, but more importantly for survivability. In all cases increasing the surface roughness through saliency increases the fluid mixing and thus improving heat transfer.

VII. Acknowledgment

The authors would like to thank the Energy Technology Partnership, NGenTec Ltd, and Motor Design for PhD funding for Yew Chuan Chong; Scottish Enterprise for funding the original proof of concept work on C-GEN; SMART Scotland, for providing funding for the 25 kW prototype; Wave Energy Scotland for providing funding for the work on the linear C-GEN machine; and the Technology Strategy Board, now Innovate UK, for funding the work on heat pipes. Finally the authors would like to acknowledge Fountain Design Ltd. for providing support in the design, build and test of all the machines used in this paper.

VIII. References

[1] J.R. Bumby and R. Martin, "Axial-flux permanent-magnet air cored generator for small-scale wind turbines.", *IEE Proc.-Electr. Power Appl.*, Vol. 152, No. 5, pp 1065-1075, September 2005

[2] J.R. Bumby, N. Stannard, J Dominy and N. McLeod, "A Permanent Magnet Generator for Small Scale Wind and Water Turbines", P*roceedings of the International Conference on Electrical Machines*, pp 1-6, 2008.

[3] M. A. Mueller, A. S. McDonald, "A Lightweight Low Speed Permanent Magnet Electrical Generator For Direct-Drive Wind Turbines", *Journal Of Wind Energy (Wiley)*, Vol. 12, No. 8, 11.2009, p. 768–780.

[4] N. Hodgins, O. Keysan, A. McDonald, M. Mueller, "Design and Testing of a Linear Generator for Wave Energy Applications", *IEEE Transactions on Industrial Electronics*, Vol. 59, Issue 5, ,pp 2094-2103, 2012

[5] A. S. McDonald, N. Al-Khayat, M. Benatmane, D. Belshaw, M. Ravilious, K. Kumaraperumal, M. Galbraith, D. Staton, C. Benoit & M. A. Mueller, "1MW Multi-stage air cored permanent magnet generator for wind turbines", *6th IET International Conference on Power Electronics, Machines & Drives*, Bristol, pp 1-6, April 2012.

[6] Y C Chong, J. P. Echenique Subiabre, M. A. Mueller, J. Chick, D. A. Staton, and A. S. McDonald, "The Ventilation Effect on Stator Convective Heat Transfer of an Axial-Flux Permanent-Magnet Machine", *IEEE Transactions on Industrial Electronics*, vol. 61, no. 8, pp 4392-4403, August 2014

[7] P. H. Mellor, "Estimation of parameters and performance of rare-earth permanent-magnet motors avoiding measurement of load angle," in *Proc.Inst. Elect. Eng.—B Elect. Power Appl.,* Nov. 1991, vol. 138, no. 6,pp. 322–330.

[8] Starccmhttps://mdx.plm.automation.siemens.com/star-ccm-plus (last accessed 27th January 2018)

[9] Y. C. Chong, "Thermal analysis and air flow modelling of electrical machines." PhD thesis, University of Edinburgh, June 2015,https://www.era.lib.ed.ac.uk/handle/1842/10466?show=fullr

Prof Mueller received the B.Sc. (Eng.) degree from Imperial College London, and a Ph.D. from the University of Cambridge, in 1988 and 1991, respectively. He was a Lecturer with the School of Engineering, University of Durham, from 1997 to 2004. Since 2004, he has been with the School of Engineering, University of Edinburgh, where he holds a Personal Chair in Electrical Generation Systems and was Head of the Institute for Energy Systems, 2014-2018.

Joseph Burchell graduated from the University of Edinburgh with an MEng in Mechanical Engineering with Renewable Energy. He returned to the School of Engineering, Institute for Energy Systems to undertake his PhD in Superconducting Machines for Direct Drive Offshore Wind Turbines. He is currently working within the Institute for Energy Systems as a Research Associate undertaking a Wave Energy Scotland Project.

Dr. Keysan obtain a Masters degree from Middle Eastern Technical University in Turkey,after which he studied for a PhD at the University of Edinburgh, awarded in 2014. He is now an assistant professor in Electrical-Electronics Engineering Department, METU. His research interests include renewable energy, design and Optimisation of Electrical Machines, Smart Grid, Superconducting Machines and Permanent-Magnet Machines.

Dr. Yew Chuan Chong was awarded a PhD from the University of Edinburgh in June 2015. Currently he is a design engineer at Motor Design Ltd in the UK. His main research interests are in the thermal modelling of electrical machines using both CFD modelling and lumped parameter networks.

Dr McDonald is a senior lecturer at the EPSRC Wind and Marine Energy Systems Centre for Doctoral Training, University of Strathclyde. He studied Electrical and Mechanical Engineering at the University of Durham in 2004 and completed a PhD at the School of Engineering at the University of Edinburgh in 2008. His research interests are centred on electrical generators and their application to renewable energy.

Mike Galbraith is a mechanical engineer, founder and owner of Fountain Design Ltd in County Durham in the UK. Fountain Design's core business is in the development of novel prototype machines and test rigs, having worked with a number universities, including Edinburgh, Durham, Newcastle & Lancaster.

Dr. Estanislao J. P. Echenique Subiabre was born in Rancagua, Chile. He received the B.S. and M.Sc.-(Hons.) degrees in Electrical Engineering from the Pontificia Universidad Católica de Chile, Santiago, Chile, in 2008. He was awarded a Ph.D. by the University of Edinburgh, U.K. in July 2015. His main interests include power electronics, machine control for renewable energy, and artificial intelligence applied to machine control.